Rev.Adv.Mater.Sci. 18(2008) 231-235

XRD AND TEM CHARACTERIZATION OF Al-Mg-BASED NANOCOMPOSITE ALLOYS

N. Al-Aqeeli, G. Mendoza-Suarez and R.A.L. Drew

Metals and Materials Engineering Department, McGill University, 3610 University Street, Montréal, H3A 2B2, Canada

Received: March 29, 2008

Abstract. Aluminum- and magnesium-based alloys were developed to investigate the possibility of forming light-weight nanocomposite materials. Four nanocrystalline alloys with nominal compositions $Mg_{40}Al_{60-x}Zr_x$ (x = 0, 5, 20, and 35 at. % Zr) were prepared by mechanical alloying aiming to synthesize nanocomposite materials containing nanocrystals embedded in an amorphous matrix. The addition of Zr proved to be beneficial in refining and stabilizing the nanostructure of these alloys. However, traces of oxygen contamination were detected in the XRD diffractograms upon increasing Zr content. The mechanical behavior was investigated by microhardness tests and the results showed that upon increasing Zr, hardness improves.

1. INTRODUCTION

There exists a vast interest in developing new Al-Mg alloys since they combine desirable properties of light weight and high strengths. Additionally, they have appreciable corrosion resistance granted by adding adequate amount of Al to promote the formation of a protective and continuous Al_2O_3 layer. These characteristics make these alloys potential candidates for the use in various applications which include aerospace and automotive [1].

These alloys can be processed in many routes and the choice of processing technique depends mainly on the desired departure from equilibrium and the predetermined properties that are needed in specific service environments. Mechanical alloying (MA) is one of the preferred non-equilibrium processing techniques due to its simplicity, versatility and economic viability [2]. Moreover, it is a completely solid-state processing technique in which no melting is involved for the fabrication of the alloy.

Some work has been done on the fabrication of Al-Mg alloys using MA in order to develop alloys that possess improved mechanical properties along with light weight. One of the promising routes is the fabrication of Al-Mg nanocomposite materials that hold potential of being excellent candidates in terms of structural stability and mechanical properties. Nanocomposites were first introduced in 1990 [3] and the structure comprised mainly nano fcc-Al crystallites finely distributed in an Al-based amorphous matrix. These nanocomposites showed superior mechanical properties compared to their conventional counterparts, especially at elevated temperatures.

In order to facilitate glass formability in the Al-Mg alloys, Zr is added since Mg-Al alloys do not show tendency towards amorphization rather forming metastable phases [4]. Moreover, Zr has additional advantages including enhanced fatigue corrosion cracking resistance, suppressed natural aging and promoted superplastic behavior which were attributed to the formation of Al_3Zr intermetallic phases.

The previous work on Al-Mg-Zr alloys have concentrated on liquid processing of these alloys [5]

Corresponding author: N. Al-Aqeeli, e-mail: naser.al-aqeeli@mail.mcgill.ca

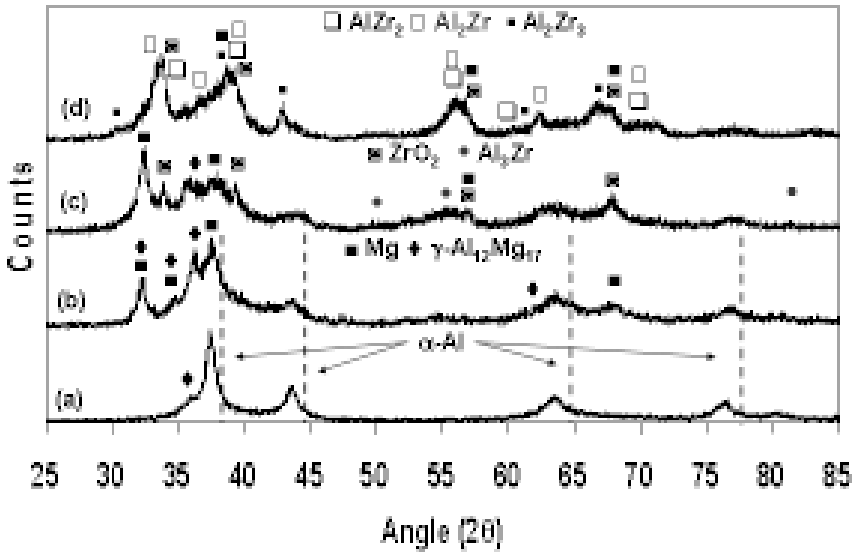

Fig. 1. XRD patterns for as-milled Al-Mg-Zr alloys with different Zr content: (a) 40Mg-60Al, (b) 40Mg-55Al-5Zr, (c) 40Mg-40Al-20Zr, (d) 40Mg-25Al-35Zr.

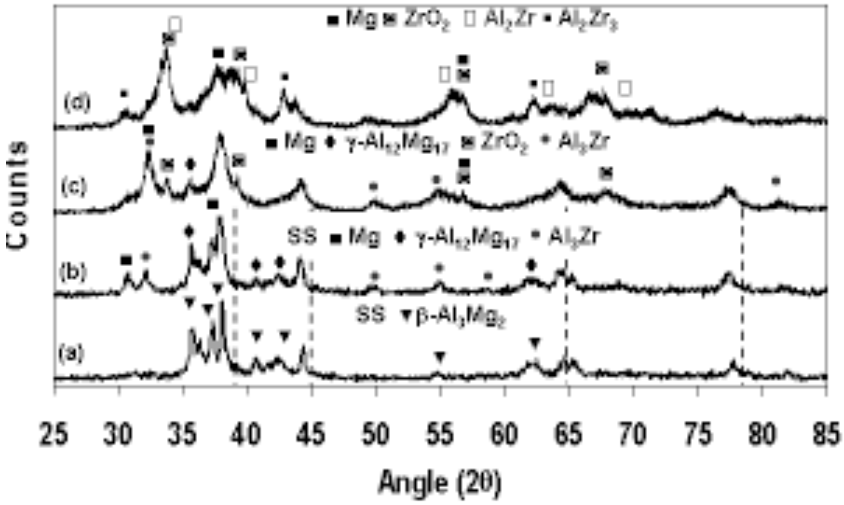

Fig. 2. XRD patterns for annealed Al-Mg-Zr alloys: (a) 40Mg-60Al, (b) 40Mg-55Al-5Zr, (c) 40Mg-40Al-20Zr, (d) 40Mg-25Al-35Zr.

with minor additions of Zr (0.1 wt.%), which proved to lead to an improvement in strength with an appreciable retention of ductility. Other investigations considered processing these alloys using MA route by adding minor amounts of Zr [6,7]; in both cases, the amounts of Zr were fixed and mainly limited to 5 and 6 at.%.

Therefore, the aim of this research is to investigate the possibility of fabricating Al-Mg-based nanocomposite alloys comprising nanocrystals embedded in an amorphous matrix using MA. In this series of alloys, the concentration of Mg was maintained at 40 at.%, to elaborate on the effect of varying Al/Zr elemental ratio on the development of the nanocomposite structure and the refinement in grain size. Hardness measurements were taken as well to evaluate any improvement in hardness due to Zr addition.

2. EXPERIMENTAL SETUP

Powder mixtures of purity >99%, -235 mesh (provided by Alfa Aesar) and nominal compositions of $Mg_{40}Al_{60-x}Zr_x$ (x = 0, 5, 20, and 35 at.% Zr) were loaded into a sealed stainless steel vial to prepare the alloys. Loading of powders was performed un-

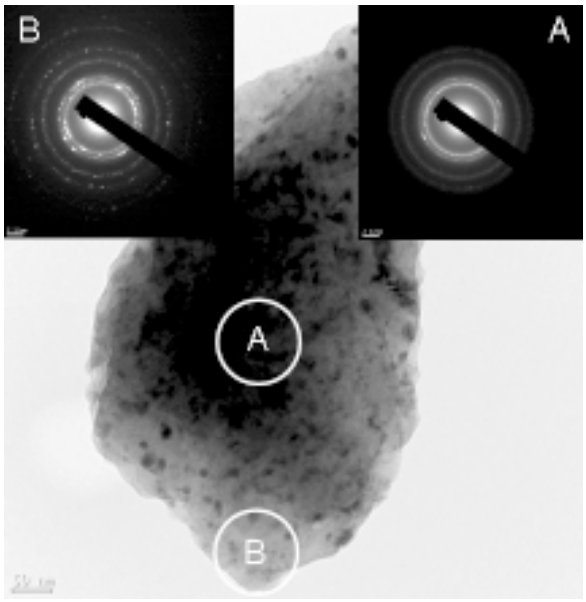

Fig. 3. TEM image and SADP of two selected areas of the Binary Al-Mg alloy showing complete crystallinity.

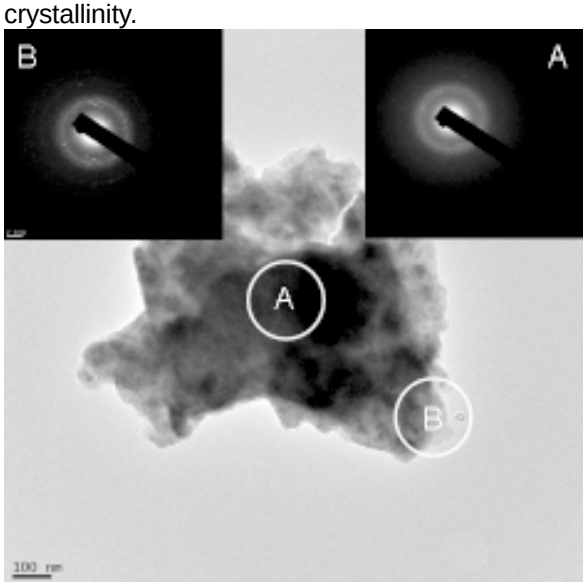

Fig. 4. TEM image and SADP of two selected areas of the 40Mg-40Al-20 at.% Zr alloy showing the presence of nanocomposite structure.

der Ar atmosphere to reduce oxygen contamination. Milling was carried out in a high-energy Spex 8000M for 9 h and ball:powder ratio (BPR) of 10 throughout the whole experiments. The milling experiments were periodically stopped every 1.5 h to avoid temperature buildup in the milling vial. Furthermore, to eliminate the accumulation of unprocessed powders on the internal walls of the vial, it was opened every 3h of milling and the deposited powders were scraped out from the vial walls. As-milled samples were annealed at 400 °C for 1h to assess thermal stability and to evaluate any possible transformations. Characterization of the resulting powders was carried out by XRD with Cu-K_α radiation and 200 kV TEM/EDS. The resulting powders were cold pressed at 1 GPa for 10 minutes, with the compaction die kept inside the hot-press for 20 minutes at 400 °C, and then pressing was carried out at 70 MPa for 10 minutes. This procedure was performed to facilitate hardness measurements which were taken using a Clark® microhardness tester.

3. RESULTS AND DISCUSSION

3.1. XRD and TEM studies

Phase evolution was characterized using XRD analyses and the patterns for as-milled alloys are shown in Fig. 1. The corresponding XRD patterns for heat-treated alloys are shown in Fig. 2. For the binary Al-Mg alloy, Al(Mg) solid solution (SS) was the main phase with traces of γ-$Al_{12}Mg_{17}$, which then transformed into the equilibrium β-Al_3Mg_2 after annealing. These results agree well with previous findings [8,9] in which the β-phase formed after annealing due to the complexity of the phase and its larger lattice parameter. This indicates that higher energies are needed to allow the formation of this phase in which the energy was supplied by heat-treatment. When Zr is added to the alloy, it forces Mg to precipitate out of SS with the consequence formation of γ-$Al_{12}Mg_{17}$. This might be related to the presence of an Al(Mg,Zr) SS, which was present post heat-treatment. The γ-phase was identified after heat-treating the alloy, which is indicative of its thermal stability. Along with that phase, Al_3Zr intermetallic also formed which is a high-temperature phase with cubic Ll_2 crystal structure, produced due to the nature of non-equilibrium processing [10]. Using equilibrium processing routes, the Al_3Zr forms in the DO_{23} tetragonal structure which is brittle and mechanical alloying shows to be beneficial in maintaining the Ll_2 cubic structure at room temperature.

When the Zr concentration was increased to 20 at.%, the SS disappeared and the only phases present were Al_3Zr along with some unalloyed Mg and traces of γ-phase. Moreover, some oxidation of Zr was detected which is attributed to the higher affinity between Zr and O. Upon annealing, the presence of unalloyed Mg, Al_3Zr and γ-$Al_{12}Mg_{17}$ was maintained. The Al-Zr intermetallic showed good thermal stability and no phase transformation was

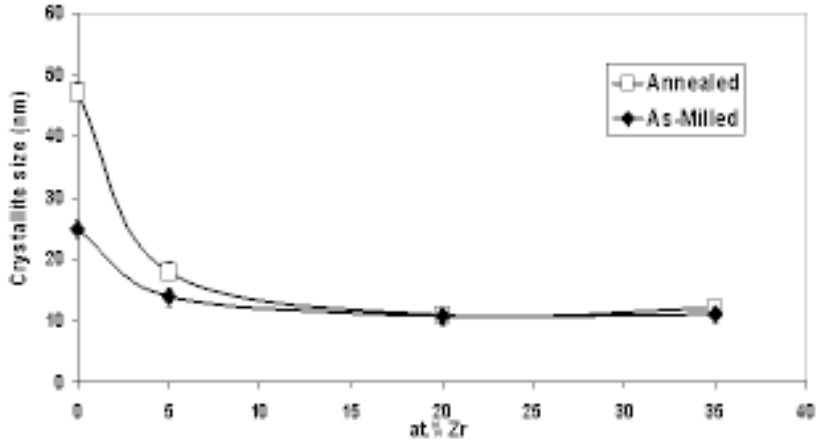

Fig. 5. Reduction in crystallite size at higher Zr concentrations.

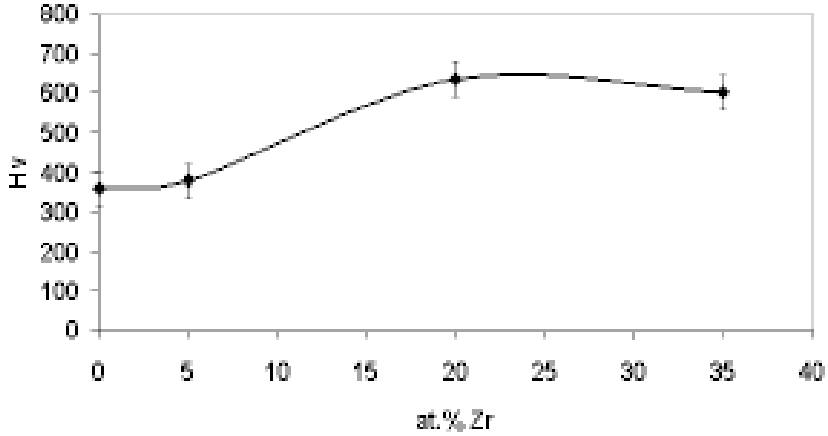

Fig. 6. Variation of hardness at different Zr concentrations.

observed. When Zr concentration was increased further to 35 at.%, some Al-Zr intermetallics appeared after milling. Some of these phases then transformed into Al_2Zr which is a more thermodynamically stable phases upon annealing, in addition to non-equilibrium $AlZr_2$ and Al_2Zr_3 phases. This might be due to the nature of the alloying process in which more deviation from equilibrium is achieved. Some unalloyed Mg and traces of ZrO_2 were observed at this composition as well. Moreover, no Al-Mg intermetallics were found to form at Zr concentrations exceeding 20 at.%, which reflects the higher stability of Al-Zr intermetallics over Al-Mg.

On the other hand, the formation of nanocomposite alloys was not confirmed from these XRD studies since partial amorphization can not be observed clearly from the X-ray diffractograms. Therefore, TEM studies were carried out for the purpose of revealing the nanocomposite structure. Fig. 3 shows a TEM image of the binary Al-Mg alloy along with selected area diffraction patterns (SADPs) of two areas. It can be seen that no amorphous phase can be detected from TEM images of this alloy. This is evident by the absence of halo-like diffractions from SADPs and the presence of clear diffraction rings. Moreover, upon the addition of 5 at.% Zr to the binary alloy there is no presence of the amorphous phase and clear diffraction rings can only be seen. For the alloys containing 20 and 35 at.% Zr, the TEM studies showed the co-existence of an amorphous phase along with some crystalline phase. The TEM image and the corresponding SADPs of the 20 at.% Zr alloy are shown in Fig. 4. By carefully examining these images, traces of amorphous phase were clear from diffraction patterns (DP) of these alloys. The nanocomposite structure was

obtained in the latter alloys, manifested by the co-existence of diffraction spots along with halo-diffraction patterns typical of an amorphous phase.

3.2. Crystallite size and hardness measurements

The determination of crystallite size was performed via direct TEM observation using Dark field (DF) images. The results for both as-milled and annealed alloys at different Zr concentrations are shown in Fig. 5. It can be seen that the crystallite size decreases as the Zr content increases for both as-milled and annealed conditions. Also, there is an apparent stability in the grain structure as the Zr content increases, manifested by the negligible grain growth for 20 and 35 at.% Zr-alloys.

Hardness measurements performed on compacted samples are shown in Fig. 6. It should be stated that upon characterizing the consolidated alloys it was observed that there was no considerable difference between annealed powders and consolidated ones. The hardness values show a continuous increase in hardness up to 20 at.% Zr where the values remained almost constant at 35 at.% Zr. The improvement in hardness might be due to the presence of the zirconium oxide that due to its hardness renders the material significantly harder. It could be related as well to the formation of the nanostructure and the presence of Al-Zr intermetallics. It is not possible to comment at this stage on the individual contribution of ZrO_2, Al-Zr intermetallics and the formation of nanocrystals on the observed improvement in hardness.

4. CONCLUSIONS

Al-Mg-Zr nanocomposite structures were obtained by adding 20 and 35 at.% Zr which promoted glass-formability, and hence facilitating the development of a partially amorphous material. For the binary alloy, some residual γ-$Al_{12}Mg_{17}$ coexisted with the Al(Mg) SS which then transformed to the equilibrium β-Al_3Mg_2 phase after heat-treatment. However, this phase was not observed after annealing the ternary alloy which further highlights the complexity of this phase. Furthermore, when Zr was added to the binary alloy, it mainly caused some Mg to precipitate out of the solid solution and form γ-$Al_{12}Mg_{17}$ along with unalloyed Mg. Upon annealing the 20 at.% Zr alloy, only the equilibrium Al_3Zr phase appeared, whereas for the 35 at.% Zr alloy the equilibrium Al_2Zr coexisted with trace amount of a high Zr-containing intermetallic (Al_2Zr_3). Oxidation occurred at 20 and 35 at.% Zr and it is attributed to the high susceptibility of Zr. However, the level of oxidation was more pronounced at 35 at.% Zr. It was observed that hardness values increases as the content of Zr increases; however it is not clear if this improvement is attributed to the presence of ZrO_2, Al-Zr intermetallics or the formation of nanocrystals.

ACKNOWLEDGEMENT

The authors acknowledge the Natural Science and Engineering Research Council of Canada (NSREC) for the support to carry out this research. The authors would like to thank Les Regroupement Aluminium (REGAL) for their funding. Acknowledgments are also due to Dr. C. Suryanarayana for fruitful discussion. The TEM work was carried out at le centre de caractérisation microscopique des matériaux at l'École Polytechnique de Montréal.

REFERENCES

[1] C. Suryanarayana, E. Ivanov and V. V. Boldyrev // *Materials Science and Engineering A* **304-306** (2001) 151.

[2] C. Suryanarayana and E. Ivanov, *Mechanical alloying for advanced materials* (Chicago, IL, United States, Minerals, Metals and Materials Society, Warrendale, PA 15086, United States,2003).

[3] Y.-H. Kim, A. Inoue and T. Masumoto // *Materials Transactions, JIM* **31** (1990) 747.

[4] D.L. Zhang // *Progress in Materials Science* **49** (2004) 537.

[5] Z. Yin, Q. Pan, Y. Zhang and F. Jiang // *Materials Science and Engineering A* **280** (2000) 151.

[6] L.E. Hazelton // *Metallurgical and Materials Transactions A* **32A** (2001) 3099.

[7] N. Al-Aqeeli, G. Mendoza-Suarez, A. Labrie and R.A.L. Drew // *Journal of Alloys and Compounds* **400** (2005) 96.

[8] D.L. Zhang, T.B. Massalski and M.R. Paruchuri // *Metallurgical and Materials Transactions A* **25A** (1994) 73.

[9] M. Schoenitz and E.L. Dreizin // *Journal of Materials Research* **18** (2003) 1827.

[10] P.B. Desch, R.B. Schwarz and P. Nash // *Journal of the Less-Common Metals* **168** (1991) 69.